J. Serb. Chem. Soc. 72 (8–9) 773–785 (2007) UDC 541.182.64+546.26+544.478:547.422+541.8
JSCS–3611 *Original scientific paper*

Characterization of a surface modified carbon cryogel and a carbon supported Pt catalyst

BILJANA M. BABIĆ[1], BRANKA V. KALUĐEROVIĆ[1], LJILJANA M VRAČAR[2], VELIMIR RADMILOVIĆ[3] and NEDELJKO V. KRSTAJIĆ[2*]

[1]*Vinča Institute of Nuclear Sciences, P.O.B. 522, 11001 Belgrade,* [2]*Faculty of Technology and Metallurgy, University of Belgrade, Karnegijeva 4, 11120 Belgrade, Serbia and* [3]*National Center for Electron Microscopy, LBLN University of California, Berkeley, USA*

(Received 27 November 2006, revised 22 January 2007)

Abstract: A carbon cryogel, synthesized by carbonization of a resorcinol/formaldehyde cryogel and oxidized in nitric acid, was used as catalyst support for Pt nanoparticles. The Pt/C catalyst was prepared by a modified polyol synthesis method in an ethylene glycol (EG) solution. Characterization by nitrogen adsorption showed that the carbon cryogel support and the Pt/C catalyst were mesoporous materials with high specific surface areas ($S_{BET} > 400$ m^2 g^{-1}) and large mesoporous volumes. X-Ray diffraction of the catalyst demonstrated the successful reduction of the Pt precursor to metallic form. TEM Images of the Pt/C catalyst and Pt particle size distribution showed that the mean Pt particle size was about 3.3 nm. Cyclic voltammetry (CV) experiments at various scan rates (from 2 to 200 mV s^{-1}) were performed in 0.5 mol dm^{-3} $HClO_4$ solution. The large capacitance of the oxidized carbon cryogel electrode, which arises from a combination of the double-layer capacitance and pseudocapacitance, associated with the participation of surface redox-type reactions was demonstrated. For the oxidized carbon cryogel, the total specific capacitance determined by $1/C$ *vs.* $v^{0.5}$ extrapolation method was found to be 386 F g^{-1}. The hydrogen oxidation reaction at the investigated Pt/C catalyst proceeded as an electrochemically reversible, two-electron direct discharge reaction.

Keywords: carbon cryogel, platinum catalyst, hydrogen oxidation, fuel cell.

INTRODUCTION

Porous carbon, due to its high surface area and pore accessibility, excellent thermal and chemical stability, as well as good electrical conductivity, is an extremely attractive and competitive material for application in electrochemistry.

Carbon aerogels and cryogels are a special class of materials,[1–4] which are usually formed from the sol–gel polycondensation of resorcinol and formaldehyde, followed by supercritical or freeze drying, and subsequent pyrolysis. The resulting carbon aerogels and cryogels are electrically conductive, in contrast to all other

* Corresponding author. E-mail: nedeljko@tmf.bg.ac.yu
doi: 10.2298/JSC0709773B

types of organic and inorganic aerogels, which are generally insulating materials. The need to control the structure and properties of porous carbon aerogels and cryogels has led to their increased use as electrode materials in advanced energy storage devices and other electrochemical devices.[5,6]

Interest in the application of a carbon aerogels as catalyst supports results from their unique electronic and morphological structure and their high surface area, the last characteristic being essential for the optimal activity of a catalyst for electrochemical reactions, since they occur on the surface of the particles. An increase in surface area of Pt/C catalyst is usually achieved by deposition of nano-sized Pt particles on a highly porous carbon support, using a variety of preparation methods.[7–12]

It is now generally accepted that the size and distribution of the catalyst particles are affected by the physical structure of the support (porosity and surface area) and the nature of the catalyst precursor. Since carbon aerogels and cryogels have a large specific surface and many unsaturated carbon atoms, these atoms react with heteroatoms from environment (O, H, N). The chemical properties of these materials arise mostly from incorporation of oxygen, forming oxides, carboxylic, phenolic, lactonic and etheric groups which are responsible for the acid/base and the redox properties of a carbon material. Surface modification (oxidation) of these materials gives a more hydrophilic surface with a relatively large number of oxygen containing surface groups.[13] Modification of the surface chemistry results in a significant change in the loading capacity. However, conflicting results concerning the influence of oxidative pretreatments of the carbon on the catalyst dispersion have regularly been reported in the literature. According to some references, for carbon supported platinum catalysts prepared by the impregnation method, both the dispersion and resistance to sintering increase with increasing number of oxygen surface groups on the support.[14–17] The opposite conclusion was also reported for similar catalytic systems, namely, that the presence of oxygen surface groups on the carbon leads to lower metal dispersions and lower resistance to sintering.[18–20]

In this article, the preparation and electrochemical characterization of a new type of oxidized carbon cryogel employed as a catalyst support for Pt nanoparticles is reported. The relation between the specific surface area of the carbon support and the particle size distribution of the Pt catalyst, as well as the effect of carbon oxygen surface groups on their dispersion and, consequently, on their catalytic activity for the hydrogen oxidation reaction were investigated.

EXPERIMENTAL

Carbon support and catalyst preparation

The carbon cryogel was sythesized by polycondensation of resorcinol and formaldehyde, according to a method described in the literature.[21] Sodium carbonate was used as the basic catalyst. The solution was prepared from resorcinol (R), (99 % purity, Merck) and formadehyde (F), 36 % methanol stabilized (Fluka Chemie), sodium carbonate (C), p.a. quality (Merck) and deionized water (W). The molar ratio between R and F was 0.5, the molar ratio between R and C was 100 and fi-

nally, the mass ratio between R and W was 20. The mixture was decanted into a glass tube, sealed and placed 2 days at 25 °C, 1 day at 50 °C and 4 days at 85 °C. The RF gel was immersed in a 10-times volume of *t*-butanol and rinsed to give the liquid contained in the gel with *t*-butanol. The sample was freeze-dried at −30 °C for 24 h. The vacuum during twenty hours of freeze-drying was around 4 mbar. The carbon cryogel was prepared by carbonization of the gel in a conventional furnace, in nitrogen flow, at 800 °C and the furnace was cooled at room temperature after pyrolysis.

To study the influence of surface oxidation, 250 mg of carbon cryogel was immersed in 50 cm^3 of 5 mol dm^{-3} HNO_3, for 3 h, at room temperature. Subsequently the sample was filtered, washed with distilled water and dried at 80 °C for 8 h.

The modified ethylene glycol method (EG) for the preparation of the Pt catalyst[22] can be described as follows: hexachloroplatinic(IV) acid (H_2PtCl_6) solution was dissolved in ethylene glycol (EG) solution containing 5 vol % of water. To adjust the pH of the solution to the value of 12, the required amount of 1.0 mol dm^{-3} NaOH (in EG) was added immediately to the EG solution. The so-prepared solution was added dropwise, under mechanical stirring to an ultrasonically dispersed carbon ethylene glycol solution. The temperature was increased to 130 °C and kept constant for 2 h in order that the platinum salt could be adequately reduced to platinum metal. The whole preparation process was conducted under a dynamic argon atmosphere. After filtration and washing, the filter cake was dried under vacuum at 60 °C for 12 h. The Pt loading of the all catalysts was always 20 wt. %. The Pt/C catalysts were finally heat-treated at 300 °C under a H_2 atmosphere for 1 h.

Characterization of the oxidized carbon cryogel and oxidized carbon cryogel with Pt nanoparticles

Adsorption and desorption isotherms of N_2 of the carbon cryogel were measured at −196 °C using the gravimetric McBain method. From the isotherms, the specific surface area, S_{BET}, pore size distribution, mesopore including external surface area, S_{meso}, and micropore volume, V_{mic}, for the samples were calculated. The pore size distribution was estimated by applying the BJH (Barret, Joyner, Halenda) method[23] to the desorption branch of the isotherms and the mesopore surface and micropore volume were estimated using the high resolution α_s plot method.[24-26] The micropore surface, S_{mic}, was calculated by subtracting S_{meso} from S_{BET}.

Oxidized carbon cryogel and C/Pt catalyst were characterized by recording their powder X-ray diffraction (XRD) patterns on a Siemens D500 X-ray diffractometer using CuKα radiation with a Ni filter. The 2θ angular regions between 5 and 80° were examined at a scan rate of 0.02° s^{-1}, with an angular resolution of 0.02°.

Transmission electron microscopy (TEM) measurements were performed at the National Center for Electron Microscopy (NCEM) using FEI (Fillips electronic instruments) CM200 super-twin and CM300 ultra-twin microscopes operating at 200 and 300 kV and equipped with the Gatan 1k×1k and 2k×2k CCD cameras, respectively. Specimens for transmission electron microscopy were prepared by suspending the catalyst powder in ethanol using an ultrasonic bath. This suspension was dropped onto clean holey carbon grids and dried in air. The particle size distributions were determined from images of, an average, 20 different regions of the catalyst; each region contained 10–20 particles. The particle shape was determined by real space crystallography using high-resolution images taken from particles near or on the edge of the carbon substrate, and/or by numerical Fourier filtering of the the digitized image intensity spectrum of particles on top of the carbon.

Cell and electrode preparation

Two milligram of sample was ultrasonically suspended in 1.0 ml of a water–methanol mixture (v/v = 1/1) and 50 μl of Nafion solution (5 wt. % Aldrich solution) to prepare a sample ink. Then, 12.5 μl of ink was transferred with an injector to a clean gold disk electrode (6 mm diameter, with an area of 0.28 cm^2). After volatilization of the water–methanol, the electrode was heated at 80 °C for 10 min.

A conventional RDE and three-compartment cell were used. The working electrode compartment was separated from the other two compartments by fritted glass discs. All measurements were

performed in 0.5 mol dm^{-3} $HClO_4$ solution (Spectrograde, Merck), prepared in highly pure water at 20 °C. The counter electrode was a platinum sheet of 5 cm^2 geometric area. A platinum plated Pt reversible hydrogen electrode (RHE) in the same solution as the working electrode was used as the reference electrode.

Electrode characterization

Electrochemical characterization was performed using an EG&G 273 instrument. Cyclic voltammetry was performed in 0.5 mol dm^{-3} $HClO_4$ saturated with high purity nitrogen which was continuously bubbled through the working electrode compartment. The CVs were recorded in the potential range from 0.03 to 1.20 V (RHE) at a rotating speed of 2500 rpm at a scan rate in the range from 2 to 200 mV s^{-1}.

RESULTS AND DISCUSSION

Adsorption isotherms – BET experiments

Nitrogen adsorption isotherms for the oxidized carbon cryogel and Pt/C catalyst, as the amount of N_2 adsorbed as function of the relative pressure at −196 °C, are shown in Fig. 1. According to the IUPAC clasification, the isotherms are of type-IV with a small hysteresis loop which is assosiated with mesoporous materials. The specific surface area, calculated by the BET equation, S_{BET}, is listed in Table I, together with the corresponding value for the non-oxidized sample, which was given in a previous paper.[21] In comparison with this result, it is obvious that surface oxidation with nitric acid leads to decrease of the overall specific surface (from 573 to 440 m^2 g^{-1}), until the process of loading of the Pt nanoparticles increased the specific surface area of the oxidized sample. On the contrary, the value of S_{BET} and mesoporous surface area of non-oxidized carbon cryogel support decreased with the addition of nano-sized Pt particles.

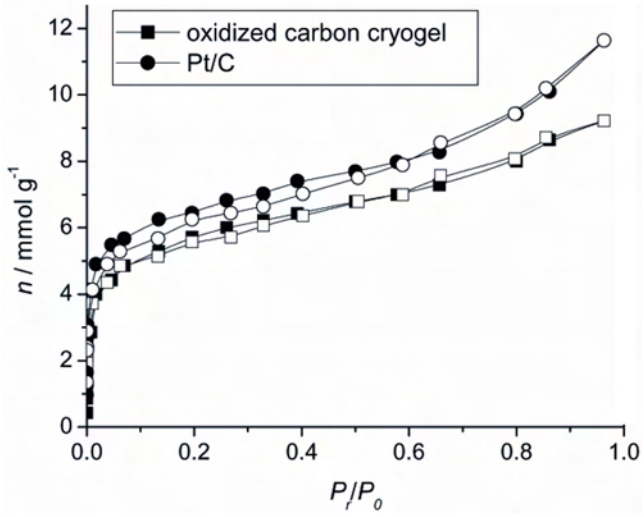

Fig. 1. Nitrogen adsorption isotherms, as the amount of N_2 adsorbed as a function of the relative pressure for oxidized carbon cryogel and Pt/C samples. Solid symbols – adsorption, open symbols – desorption.

The pore size distribution of the oxidized carbon cryogel and Pt/C samples are shown in Fig. 2. The distribution has a single peak and the value for the pore

radius of the maximum of observed curves, rpeak, was between 1–2 nm. Both samples (support and catalyst) had sharp and similar pore size distributions.

TABLE I. Porous properties of the carbon cryogel support and Pt/C samples

Sample	S_{BET} $m^2\ g^{-1}$	S_{meso} $m^2\ g^{-1}$	S_{micro} $m^2\ g^{-1}$	V_{micro} $cm^3\ g^{-1}$	C_{tot} $F\ g^{-1}$
Oxidized carbon cryogel	440	145	295	0.14	386
Oxidized carbon cryogel + 20 wt. % Pt	501	185	316	0.15	–
Non-oxidized carbon cryogel[21]	573	258	315	0.15	124
Non-oxidized carbon cryogel + 20 wt.% Pt	517	234	283	0.13	–

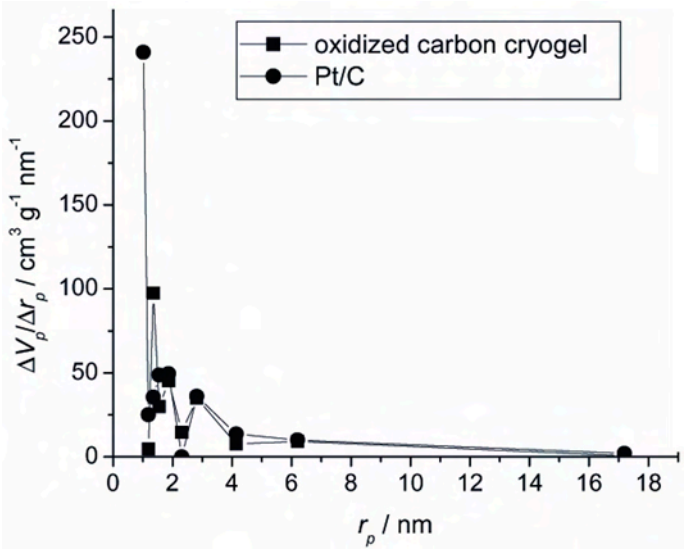

Fig. 2. Pore size distribution of the oxidized carbon cryogel and Pt/C catalyst.

The α_s plots, obtained on the basis of the standard nitrogen adsorption isotherms for the support and catalyst are shown in Fig. 3. The straight line in the medium α_s region gives a mesoporous surface area including the contribution of external surface, S_{meso}, determined by its slope, until the micropore volume, V_{mic}, is determined by the intercept. The calculated porosity parameters (S_{meso}, S_{mic} and V_{mic}) are given in Table I and they show that the mesoporous specific surface decreased as a conseqence of surface oxidation.[21] Pt loading also slightly increased mesoporous surface.

It is well known[15] that oxidation treatments of carbons lead to the formation of different surface acid groups, mainly carboxylic, anhydride, lactone, phenol and carbonyl groups. Carboxylic and anhydride groups are considered as strong acid ones, while the other ones display weaker acid properties. Moreover, it has been reported that the stronger acid groups lead to CO_2 desorption at low temperatures during temperature-programmed desorption (TPD) experiments, in contrast to the weaker acid sites which lead to CO-desorption at higher temperatures.[15] The oxida-

tive treatment of the carbon cryogel with HNO_3 solution, as was previously mentioned, results in a reduction of the specific surface area and porosity of the support.

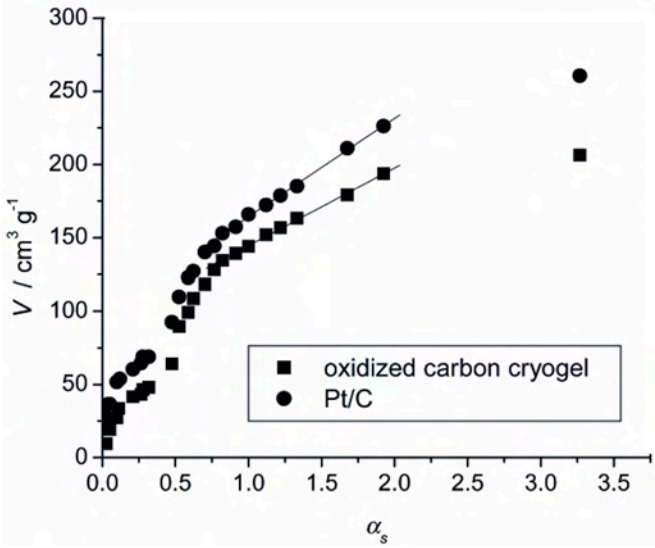

Fig. 3. α_s Plots for the nitrogen adsorption isotherm of the oxidized carbon cryogel and Pt/C catalyst, based on the standard isotherm of non-porous carbon.

During the activation process of Pt/C samples under a H_2 atmosphere at 300 °C complex processes could take place at the oxidized carbon support. Thus, the decomposition of strong acid groups into CO_2 and their transformation into CO by combination with atomic hydrogen produced by dissociation of H_2 on the metallic Pt particles.[15] The increase in the porosity and specific surface are of the oxidized carbon cryogel sample after Pt loading and the final activation process could be explained by the decomposition of the oxygenated surface groups and formation of gaseous products (CO_2 and CO), which increase the pore volume.

XRD Analysis of Pt catalyst

The XRD patterns of the oxidized carbon cryogel and the Pt/C samples are shown in Fig. 4. XRD Pattern of the oxidized carbon cryogel, *i.e.*, without characteristic peaks, proves the amorphous structure of the carbon material. The characteristic diffraction peaks of face centered cubic (fcc) phase Pt for the Pt/C catalyst demonstrate that a successful reduction of the Pt precursor to metallic Pt had been achieved. The diffraction peaks at about 39° and 46°, due to the Pt (111) and (200) plane, respectively, represent the typical character of a crystalline Pt face that is a fcc phase. There are no other distinct reflection peaks in all patterns in the investigated 2θ range than the two peaks already mentioned above, indicating that in these in-house supported Pt catalysts, the Pt fcc crystal structure prevailed.

TEM Analysis

The low magnification TEM micrograph (Fig. 5) shows a very uniform size distribution of the Pt particles, with a mean particle size of about 3.3 nm. The hi-

stogram of Pt particle size distribution of Pt/C catalyst was obtained based on measurements of over 300 Pt particles.

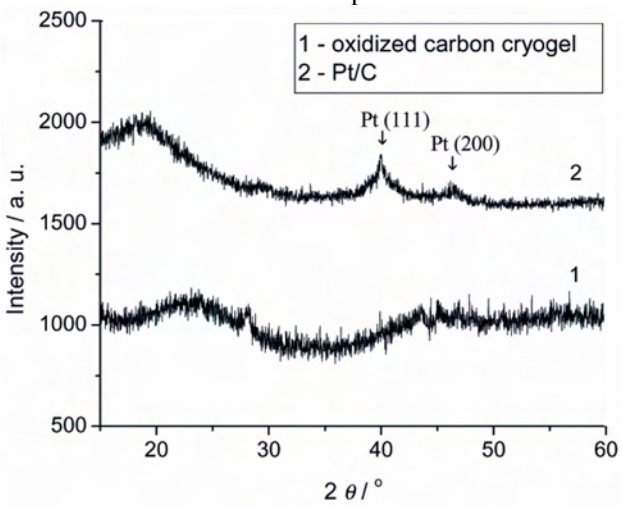

Fig. 4. XRD Patterns of the oxidized carbon cryogel and Pt/C catalyst.

The atomically resolved image in Fig. 6 shows rows of Pt atoms with a spacing corresponding to the (200) and (111) planes of the face centered cubic Pt nanoparticles, as indicated in the corresponding digital diffractograms, also shown in Fig. 6. The Pt particles have the common cubo-octahedral shapes. Twinned particles were observed occasionally with the same (111) twinning plane as in some other Pt based catalysts.[27]

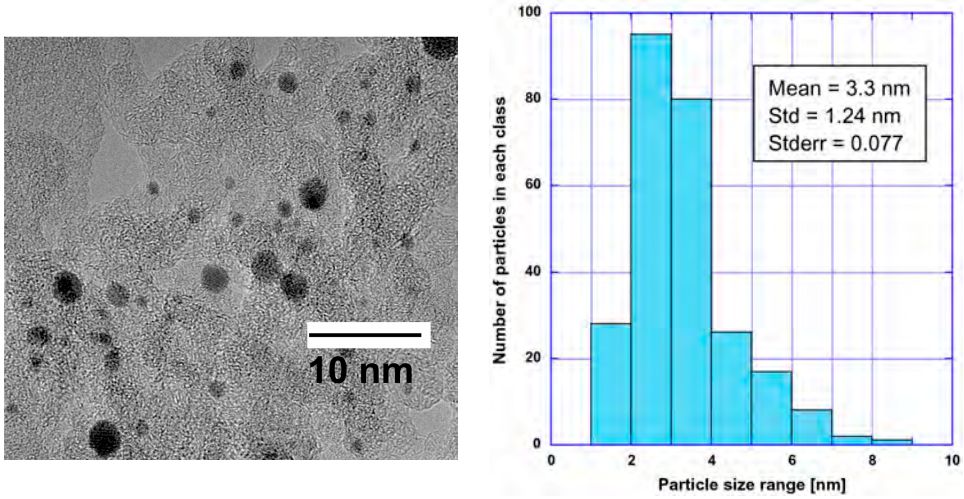

Fig. 5. TEM Micrographs of Pt nanoparticles on the oxidized carbon cryogel (Pt/C catalyst). The lower magnification shows the spread of the Pt particle size distribution.
The corresponding size histogram is also shown.

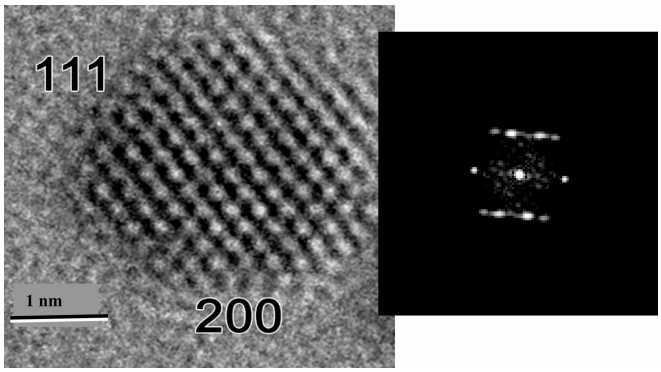

Fig. 6. High resolution image showing one-dimensional lattice fringes of the (111) lattice planes in Pt.

Cyclic voltammetry experiments

Cyclic voltammograms (CV) of the oxidized carbon cryogel (C) and Pt/C samples, at different scan rates (2–200 mV s^{-1}) are shown in Figs. 7a and 7b, respectively. The cyclic voltammetry experiments showed that, due to the oxidation process, the basic voltammogram is different from that observed for a non-oxidized carbon cryogel.[21] The voltammograms of the oxidized sample show, to some extent, deviation from a rectangular shape and the presence of reversible redox peaks connected with pseudo-Faradic reactions. Chemical treatment of the carbon cryogel with nitric acid significantly increased the voltametric charge. Although the oxidation process decreased the specific surface, the overall voltametric charge increased remarkably due to redox processes of the functional groups on the surface (pseudocapacitance).

The specific capacitance decreased with increasing the scan rate (Fig. 7). It was shown[21] that the voltammetric charge and/or capacitance, should be a linear function of $\nu^{-0.5}$ and the reciprocal capacitance should be a linear function of $\nu^{0.5}$. The extrapolation of the $1/C - \nu^{0.5}$ line to $\nu^{0.5} \rightarrow 0$ gives the capacitance at an infinity slow scan rate, *i.e.*, under the conditions of reversibility. Under the condition of a slow scan rate, it was assumed that the charging process is able to reach equilibrium at the whole surface (external and internal), meaning that the specific capacitance measured at this scan rate corresponds to the total capacitance. For the oxidized carbon cryogel, the so-determined total specific capacitance was found to be 386 F g^{-1} (the total specific capacitance of the non-oxidized carbon cryogel was 124 F g^{-1}). Literature data show that the specific capacitances of other carbon materials[28–33] are significantly lower than the present measured value and for this reason the present result could be very important for further investigations and applications of surface modified carbon cryogels in supercapacitors.

Cyclic voltammetry measurements on the Pt/C electrode were performed to determine the electrochemical surface area of the Pt and to elucidate the adsorption properties of the catalyst. The electrochemically active surface area of the ca-

talyst was calculated from the charge associated with the anodic desorption peak of underpotential deposited (UPD) hydrogen at the Pt nano-sized particles. The base line was taken by extrapolation of the double-layer region of the voltammogram. The electrochemically active surface area of the catalysts (S_{easa}) was calculated from the measured charge assuming 210 μC cm^{-2} as the charge of full coverage with adsorbed hydrogen. The electrochemical surface area for this electrocatalyst was found to be 2.36 cm^2 (47 m^2 g^{-1}).

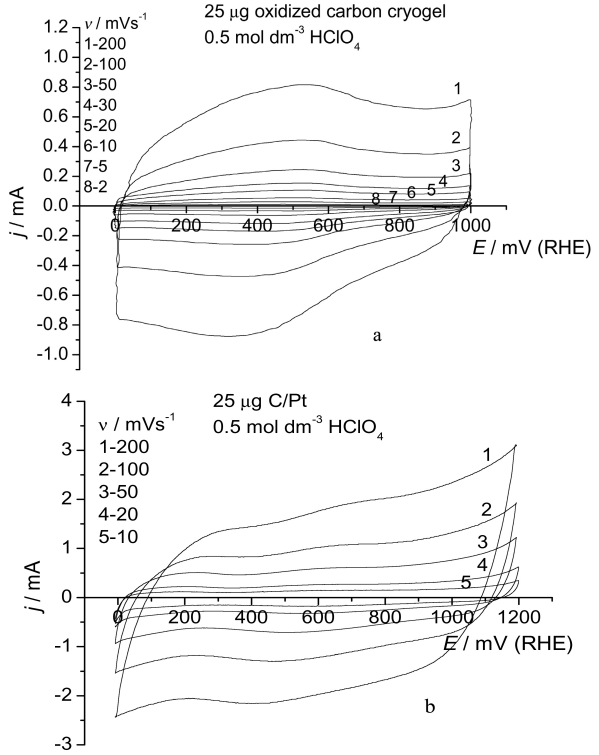

Fig. 7. Cyclic voltammograms of the oxidized carbon cryogel and Pt/C catalyst a) oxidized carbon cryogel b) Pt/C in 0.5 mol dm^{-3} $HClO_4$ solution at 293 K.

The total surface area of Pt catalyst, S_{tot}, was calculated from the corresponding values of the mean particle size, d, and the density of Pt metal, $\rho = 4.24$ cm^2. The Pt utilization efficiency for the RDE was determined using the following equation: $Pt_{u.e.} = S_{easa} / S_{tot}$. The Pt utilization efficiency was 56 %. However, the Pt utilization efficiency on the non-oxidized carbon cryogel support was around 88 %.[21] This means that the presence of carboxyl surface groups on the oxidized carbon cryogel support, under the present conditions, results in a lower utilization efficiency and a lower metal dispersion during the reduction of the anionic precursor, $PtCl_6^{2-}$ in ethylene glycol at 130 °C. Electrostatic repulsion between the anionic entities and the acid groups of the oxidized carbon support can explain the low dispersion of Pt particles. This interpretation is in line with that proposed for a series of Pt catalysts supported on graphitized carbon blacks.[15] The-

se results also indicate that the control of the final metallic dispersion of a high surface area carbon-supported Pt catalyst also depends on the presence of oxygen surface groups on the carbon support.

Kinetics of the hydrogen oxidation at the Pt/C catalyst

The hydrogen oxidation polarization curves for several rotation speeds, obtained at a scan rate of 2 mV s^{-1} in 0.5 mol dm^{-3} $HClO_4$ solution, on the Pt/C electrode are presented in Fig. 8. The current is increased rapidly with potential on each curve, reaching a limiting value at a potential of *ca*. 60 mV (RHE).

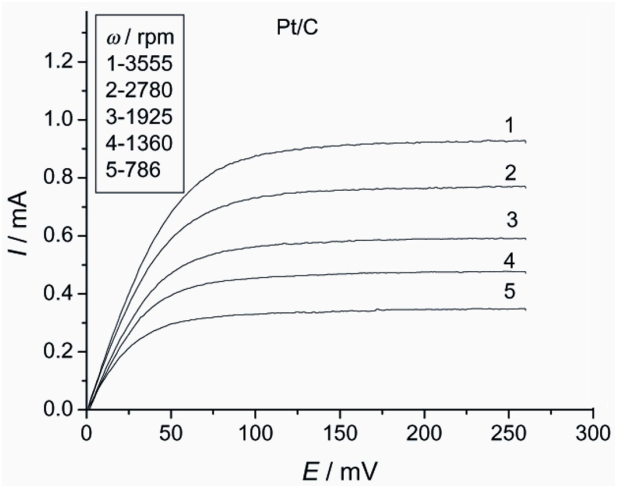

Fig. 8. Current *vs*. potential curves of the electrocatalytic oxidation of H_2 on the Pt/C catalyst (T = 293 K, v = 2 mV s^{-1}), on RDE electrode, in 0.5 mol dm^{-3} $HClO_4$ solution under a H_2 atmosphere.

In order to obtain information about the kinetics of the HOR on the investigated electrode, the RDE polarization data were analyzed in terms of mass transport corrected Tafel diagrams. The kinetic equations used for such an analysis were derived considering the reversible or irreversible nature of the electrochemical reaction.

The kinetic equations for a reversible and an irreversible electrochemical reaction[34] can respectively be given as:

$$E = E_1^{\ominus} - \frac{2.303RT}{nF}\log\left(\frac{I_D - I}{I_D}\right) \quad (1)$$

$$E = E_2^{\ominus} + \frac{2.303RT}{\alpha nF}\log\left(\frac{I_D I}{I_D - I}\right) \quad (2)$$

where $E_1^{\ominus}$ and $E_2^{\ominus}$ are current independent constants and α is the charge transfer coefficient. Equation (1) is used to obtain mass transport corrected Tafel diagrams if the reaction is assumed to be reversible, while Eq. (2) is employed to obtain mass transport corrected Tafel diagrams if the reaction is irreversible. If one or another condition is satisfied, according to Eqs. (1) or (2), the plots E – log $[(I_L–I)/I_L]$

or $E - \log [I_L \times I/(I_L - I)]$, respectively, should be linear with the points independent of the rotation rate.

It is clear that linear plots practically independent of the rotation speed were obtained when reversible kinetic were assumed (Fig. 9). The slope of the linear plot is very close to the theoretical value of 29 mV dec^{-1}. However, there is no agreement with the prediction of Eq. (2). In this case, the linear relationship of $E - \log [I_L \times I/(I_L - I)]$ is also established in the potential range where the correction for the reverse reaction is not necessary, but the linear plots depend on the rotation speed and the slopes are around 28 mV dec^{-1}, which is only half of the predicted value of 58 mV dec^{-1}. Therefore, the most reasonable assumption that electrochemical hydrogen oxidation reaction at the investigated Pt/C catalyst is reversible seems to be experimentally justified.

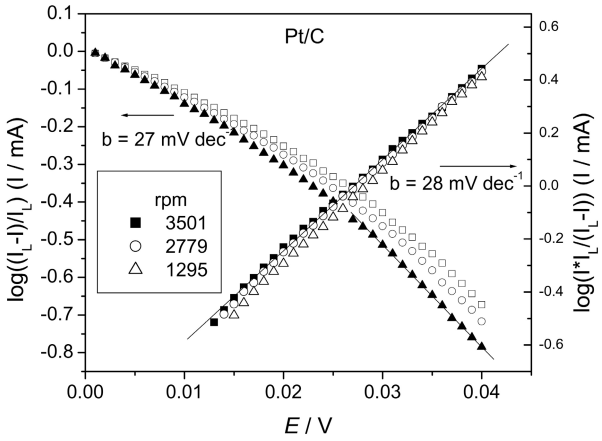

Fig. 9. Plots of $E - \log [(I_L - I)/I_L]$ and $E - \log [I_L \times I/(I_L - I)]$. Data taken from the RDE plots in Fig. 8.

The mechanism of the HOR has been extensively studied in acidic and base solutions.[35,36] The chance of extracting 2 e$^-$ directly from H_2 in a direct discharge reaction is usually considered low. However, the kinetic analysis conducted in this paper shows that the HOR occurs as a reversible two-electron direct discharge reaction at the investigated Pt/C catalyst.

CONCLUSION

The effect of the specific surface area and oxygen surface groups of a carbon support on the catalytic properties of Pt/C were investigated using an oxidized carbon cryogel. The catalyst was prepared by a modified polyol synthesis method and heat-treatment under a hydrogen atmosphere at 300 °C. The results show that the specific surface area of the oxidized carbon cryogel support (S_{BET}) decreases after oxidation with HNO_3. However, the calculated total specific capacitance determined from CV experiments significantly increased from 124 to 386 F g^{-1} due to oxidative–reductive processes on the surface functional groups (pseudocapacitance).

The presence of oxygen surface groups on the carbon led to low metal dispersions and utilization efficiency (56 %). The mean Pt particle size on the oxidi-

zed carbon cryogel was 3.3 nm. These results also indicate that the control of the final metallic dispersion of a high surface area, carbon-supported metal catalyst depends also on the presence of oxygen surface groups on the carbon support.

Analysis of the hydrogen oxidation reaction showed that this reaction occurs at the investigated Pt/C catalyst as a reversible two-electron direct discharge reaction.

Acknowledgements: This study was supported by the Ministry of Science of the Republic of Serbia, under Contracts No. 142016 and 142038 and partially by the Office of Basic Energy Sciences of the U.S. Department of Energy under contract No. DE–AC0376SF00098.

И З В О Д

КАРАКТЕРИЗАЦИЈА ПОВРШИНСКИ МОДИФИКОВАНОГ УГЉЕНИЧНОГ КРИОГЕЛА И ПЛАТИНА/УГЉЕНИК КАТАЛИЗАТОРА

БИЉАНА М. БАБИЋ[1], БРАНКА В. КАЛУЂЕРОВИЋ[1], ЉИЉАНА М. ВРАЧАР[2], ВЕЛИМИР РАДМИЛОВИЋ[3] и НЕДЕЉКО В. КРСТАЈИЋ[2]

[1]Институт за нуклерне науке "Винча", п. пр. 522, 11000 Београд, [2]Технолошко–металуршки факултет, Карнегијева 4, 11120 Београд и [3]National Center for Electron Microscopy, LBLN University of California, Berkeley, USA

Угљенични криогел, синтетизован карбонизацијом резорцинол/формалдехид криогела и оксидован у азотној киселини употребљен је као носач катализатора за наночестице платине. Платина/угљеник катализатор припремљен је модификованом полиол методом, у раствору етилен-гликола. Карактеризација адсорпцијом азота показала је да су угљенични криогел и платина/угљеник катализатор мезопорозни материјали високе специфичне површине (> 400 $m^2\ g^{-1}$) и мезопорозне запремине. Метода рентгенске дифракције показала је да је постигнута редукција прекурсора платине до металног облика. TEM анализа платина/угљеник катализатора и расподела величине честица платине показује да је средњи пречник честица око 3,3 nm. Испитивања методом цикличне волтаметрије, при различитим брзинама промене потенцијала (2 – 200 mV s^{-1}), показала су да електрода од оксидованог угљеничног криогела има веома висок капацитет који потиче од комбинације капацитета двојног слоја и псеудокапацитета. Укупан специфични капацитет оксидованог угљеничног криогела износи 386 F g^{-1}. Реакција оксидације водоника на наночестицама платине одвија се по механизму реверзибилне директне оксидације.

(Примљено 27. новембра 2006, ревидирано 22. јануара 2007)

REFERENCES

1. R. W. Pekala, *J. Matter. Sci.* **24** (1989) 3221
2. R. W. Pekala, C. T. Alviso, X. Lu, J. Gross, *J. Non–Cryst. Solids* **188** (1995) 34
3. H. Tamon, H. Ishizaka, T. Yamamoto, T. Suzuki, *Carbon* **37** (1999) 2049
4. T. Yamamoto, T. Sugimoto. T. Suzuki, S. R. Mukai, H. Tamon, *Carbon* **40** (2002) 1345
5. B. Babić, D. Đokić, N. Krstajić, *J.Serb.Chem.Soc.* **70** (2005) 21
6. K. L. Yang, S. Yiacuomi, C. Tsouris, *J. Electroanal. Chem.* **540** (2003) 159
7. Y. Yang, Y. Zhou, C. Cha, W. M. Carrol, *Electrochim. Acta* **38** (1993) 2333
8. Y. Gao, F. Naguchi, T. Mitamura, H. Kita, *Electrochim. Acta* **37** (1992) 1327
9. Y. Takusu, N. Ohashi, X.–G. Zhang, Y. Murukami, H. Minagawa, S. Sato, K. Yahikozawa, *Electrochim. Acta* **41** (1996) 2595
10. S. Hirano, J. Kim, S. Srinivasan, *Electrochim. Acta* **42** (1997) 1587

11. M. T. Reetz, W. Helbig, *J. Am. Chem. Soc.* **116** (1994) 7401
12. C. Prado–Burguete, A. Linares–Solano, F. Rodrìguez–Reinoso, C. S. M de Lecea, *J. Catal.* **115** (1989) 98
13. Lj. R. Radović, F. Rodriges–Reinoso, in *Chemistry and Physics of Carbon*, P. A. Thrower, Ed., Dekker, New York, Vol. 25 (1996) p. 243
14. G. C. Torres, E. L. Jablonski, G. T. Baronetti, A. A. Castro, S. R. de Miguel, O. A. Scelza, M. D. Blanco, M. A. Peña Jiménez, J. L. G Fierro, *Appl. Catal. A* **161** (1997) 213
15. S. R. de Miguel, O. A. Scelza, M. C. Román–Martìnez, C. S. M de Lecea, D. Cazorla–Amoros, A. Linares–Solano, *Appl. Catal. A* **170** (1998) 93
16. D. J. Suh., T. J. Park, S. K. Ihm, *Carbon* **31** (1993) 427
17. F. Coloma, A. Sepúlveda–Escribano, J. L. Fierro, F. Rodriguez–Reinoso, *Langmuir* **10** (1994) 750
18. M. C. Román–Martinez, D. Cazorla–Amorós, A. Linares–Solano, C. S. M. Lecea, *Carbon* **33** (1995) 3
19. P. Ehrburger, O. P. Majahan, P. L. Walker, *J. Catal.* **43** (1976) 61
20. A. Guerrero–Ruiz, P. Badenes, I. Rodríguez–Ramos, *Appl. Catal. A* **173** (1998) 313
21. B. Babić, B. Kaluđerović, Lj. Vračar, N. Krstajić, *Carbon* **42** (2004) 2617
22. B. M. Babić, Lj. M. Vračar, V. Radmilović, N. V. Krstajić, *Electrochim. Acta* **51** (2006) 3820
23. E. P. Barret, L. G. Joyner, P. P. Halenda, *J. Am. Chem. Soc*. **73** (1951) 373
24. K. Kaneko, C. Ishii, M. Ruike, H. Kuwabara, *Carbon* **30** (1992) 1075
25. M. Kruk, M. Jaroniec, K. P. Gadakaree, *J. Colloid Interface Sci.* **192** (1997) 250
26. K. Kaneko, C. Ishii, H. Kanoh, Y. Hanzawa, N. Setoyama, T. Suzuki, *Adv. Coll. Interface Sci.* **76–77** (1998) 295
27. V. Radmilovic, T. J. Richardson, S. J. Chen, P. N. Ross, *J. Catal*. **232** (2005) 199
28. W. Li, G. Reichenauer, J. Fricke, *Carbon* **40** (2002) 2955
29. W. Li, H. Probstle, J. Fricke, *J. Non–Cryst. Solids* **325** (2003) 1
30. J. M. Miller, B. Dunn, T. D. Tran, R. W. Pekala, *J. Electrochem. Soc*. **144** (1997) L309
31. R. W. Pekala, J. C. Farmer, C. T. Alviso, T. D. Tran, S. T. Mayer, J. M. Miller, B. Dunn, *J. Non–Cryst. Solids* **225** (1998) 74
32. C. Schmitt, H. Probstle, J. Fricke, *J. Non–Cryst. Solids* **285** (2001) 277
33. H. Probstle, C. Schmitt, J. Fricke, *J. Power Sources* **105** (2002) 189
34. A. J. Bard, L. Faulkner, *Electrochemical Methods, Fundamentals and Applications*, Ch. 8, John Wiley & Sons, New York, 1981, p.256
35. N. M. Marković, B. N. Grgur, P. N. Ross, *J. Phys. Chem. B* **101** (1997) 5405
36. N. M. Marković, T. S. Sarraf, H. A. Gasteiger, P. N. Ross, *J. Chem. Soc. Faraday Trans.* **92** (1996) 3719.